

## Supporting Information

**Bacterial Biofilm Material Properties Enable Removal and Transfer by Capillary Peeling**

Jing Yan, Alexis Moreau, Sepideh Khodaparast, Antonio Perazzo, Jie Feng, Chenyi Fei, Sheng Mao, Sampriti Mukherjee, Andrej Košmrlj, Ned S. Wingreen, Bonnie L. Bassler\*, Howard A. Stone\*

**Table S1. Summary of measured rheological properties of *V. cholerae* biofilms.**

<i>V. cholerae</i> Strain	Agar Conc. <sup>a)</sup>	Parameters			Comments
		$G'_p$ /kPa	$\epsilon_Y$	$\sigma_Y$ /kPa	
WT	0.6%	1.11 ± 0.16	0.13 ± 0.05	0.10 ± 0.03	With dual networks
	0.8%	1.16 ± 0.30	0.15 ± 0.00	0.12 ± 0.03	
	1.0%	1.12 ± 0.18	0.15 ± 0.07	0.14 ± 0.07	
	1.5%	1.38 ± 0.07	0.17 ± 0.03	0.17 ± 0.03	
$\Delta rbmA$	0.6%	0.59 ± 0.12	0.18 ± 0.02	0.08 ± 0.02	With crosslinked polymer network only
	0.8%	0.54 ± 0.10	0.20 ± 0.02	0.09 ± 0.01	
	1.0%	0.42 ± 0.11	0.27 ± 0.04	0.09 ± 0.01	
	1.5%	0.70 ± 0.04	0.27 ± 0.03	0.15 ± 0.01	
$\Delta bapI$ $\Delta rbmC$	0.6%	0.76 ± 0.15	0.10 ± 0.01	0.05 ± 0.02	With cellular network only
	0.8%	1.14 ± 0.05	0.09 ± 0.02	0.08 ± 0.01	
	1.0%	1.30 ± 0.12	0.13 ± 0.01	0.13 ± 0.01	
	1.5%	1.63 ± 0.12	0.18 ± 0.02	0.21 ± 0.02	
$\Delta rbmA$ $\Delta bapI$ $\Delta rbmC$	0.6%	0.11 ± 0.02	0.38 ± 0.01	0.03 ± 0.00	With non-crosslinked polymer network only
	0.8%	0.20 ± 0.02	0.36 ± 0.01	0.05 ± 0.00	
	1.0%	0.31 ± 0.04	0.35 ± 0.02	0.07 ± 0.00	
	1.5%	0.69 ± 0.05	0.28 ± 0.01	0.14 ± 0.01	
$\Delta vpsL$	0.6%	0.23 ± 0.10	0.15 ± 0.02	0.02 ± 0.01	No polymer network, accessory matrix proteins nonfunctional
	0.8%	0.43 ± 0.12	0.13 ± 0.00	0.04 ± 0.01	
	1.0%	0.67 ± 0.10	0.13 ± 0.00	0.06 ± 0.01	
	1.5%	1.13 ± 0.25	0.15 ± 0.02	0.12 ± 0.04	
$\Delta rbmA$ $\Delta vpsL$	0.6%	0.14 ± 0.05	0.12 ± 0.02	0.01 ± 0.00	No polymer network, accessory matrix proteins nonfunctional
	0.8%	0.29 ± 0.01	0.11 ± 0.02	0.02 ± 0.00	
	1.0%	0.45 ± 0.08	0.12 ± 0.01	0.03 ± 0.01	
	1.5%	1.04 ± 0.13	0.13 ± 0.00	0.10 ± 0.04	
$\Delta rbmA$ $\Delta bapI$ $\Delta rbmC$ $\Delta vpsL$	0.6%	0.12 ± 0.06	0.13 ± 0.05	0.01 ± 0.00	No polymer network, no accessory matrix proteins
	0.8%	0.23 ± 0.06	0.11 ± 0.02	0.02 ± 0.00	
	1.0%	0.36 ± 0.09	0.12 ± 0.02	0.04 ± 0.01	
	1.5%	0.90 ± 0.24	0.14 ± 0.03	0.11 ± 0.01	

a) Abbreviation for agar concentration in the substrate.

**Table S2. Summary of measured contact angles for surface energy calculations.**

<i>V. cholerae</i> Strain	Agar Conc. <sup>d)</sup>	H <sub>2</sub> O	CH <sub>2</sub> I <sub>2</sub>	Liquid 1-Br-NP <sup>e)</sup>	1-Me-NP <sup>f)</sup>	CH <sub>2</sub> Br <sub>2</sub>
WT	0.6%	109 ± 4°	54 ± 2°	35 ± 4°	27 ± 2°	16 ± 2°
WT	0.8%	105 ± 3°	57 ± 1°	35 ± 1°	28 ± 1°	14 ± 3°
WT	1.0%	111 ± 10°	56 ± 3°	35 ± 4°	26 ± 1°	18 ± 2°
WT	1.5%	105 ± 6°	59 ± 4°	42 ± 3°	28 ± 1°	17 ± 3°
$\Delta bapI$ <sup>a)</sup>	1.5%	31 ± 4°	76 ± 4°	N/A	N/A	N/A
$\Delta bapI\Delta rbcC$ <sup>b)</sup>	1.5%	11 ± 1°	70 ± 4°	N/A	N/A	N/A
$\Delta vpsL$ <sup>c)</sup>	1.5%	21 ± 1°	68 ± 2°	N/A	N/A	N/A

- a) Strain lacking a key surface-active matrix protein.
- b) Strain lacking two key surface-active matrix proteins.
- c) Strain lacking the key matrix polysaccharide.
- d) Abbreviation for agar concentration in the substrate.
- e) Abbreviation for 1-bromonaphthalene.
- f) Abbreviation for 1-methylnaphthalene.

Table S3. Bacterial strains and plasmids used in this study.

Strains/plasmids	Relevant Features	Reference
<b><i>E. coli</i></b>		
S17 $\lambda$ - <i>pir</i>	Wild Type	[1]
DH5 $\alpha$	F <sup>-</sup> <i>endA1 glnV44 thi-1 recA1 relA1 gyrA96 deoR nupG purB20</i>	Laboratory stock
SM10 $\lambda$ <i>pir</i>	$\phi$ 80 <i>dlacZ</i> $\Delta$ M15 $\Delta$ ( <i>lacZYA-argF</i> ) U169, <i>hsdR17(r<sub>K</sub><sup>-</sup>m<sub>K</sub><sup>+</sup>)</i> , $\lambda$ <sup>-</sup> <i>thi thr leu tonA lacY supE recA::RP4-2-Tc::Mu</i>	Laboratory stock
<b><i>V. cholerae</i></b>		
C6706 <i>str2</i>	El Tor Wild Type	[2]
JY283	<i>vpvC</i> <sup>W240R</sup> $\Delta$ <i>pomA</i> (denoted WT)	[3]
JY284	<i>vpvC</i> <sup>W240R</sup> $\Delta$ <i>pomA</i> $\Delta$ <i>rbmA</i>	[3]
JY285	<i>vpvC</i> <sup>W240R</sup> $\Delta$ <i>pomA</i> $\Delta$ <i>bapI</i> $\Delta$ <i>rbmC</i>	[3]
JY286	<i>vpvC</i> <sup>W240R</sup> $\Delta$ <i>pomA</i> $\Delta$ <i>rbmA</i> $\Delta$ <i>bapI</i> $\Delta$ <i>rbmC</i>	[3]
JY287	<i>vpvC</i> <sup>W240R</sup> $\Delta$ <i>pomA</i> $\Delta$ <i>vpsL</i>	[3]
JY288	<i>vpvC</i> <sup>W240R</sup> $\Delta$ <i>pomA</i> $\Delta$ <i>rbmA</i> $\Delta$ <i>vpsL</i>	This study
JY290	<i>vpvC</i> <sup>W240R</sup> $\Delta$ <i>pomA</i> $\Delta$ <i>rbmA</i> $\Delta$ <i>bapI</i> $\Delta$ <i>rbmC</i> $\Delta$ <i>vpsL</i>	This study
JY370	<i>vpvC</i> <sup>W240R</sup> $\Delta$ <i>pomA lacZ:P<sub>tac</sub>-mKate2:lacZ</i>	[3]
JY393	<i>vpvC</i> <sup>W240R</sup> $\Delta$ <i>pomA</i> $\Delta$ <i>rbmC</i>	[3]
JY400	<i>vpvC</i> <sup>W240R</sup> $\Delta$ <i>pomA</i> $\Delta$ <i>bapI</i>	[3]
<b><i>P. aeruginosa</i></b>		
UCBPP-PA14	Wild Type	Laboratory stock
SM404	$\Delta$ <i>pelA</i>	[4]
SM1141	$\Delta$ <i>P<sub>pelA</sub>::P<sub>hyspank</sub>-pelABCDEFG</i>	This study
<b>Plasmid</b>		
pKAS32	Suicide vector, Amp <sup>R</sup> Sm <sup>S</sup>	[5]
pNUT144	Suicide vector, Amp <sup>R</sup> Kan <sup>R</sup> Sm <sup>S</sup>	[6]
pNUT157	pNUT144 <i>vpvC</i> <sup>W240R</sup>	[6]
pCMW112	pKAS32 $\Delta$ <i>vpsL</i>	[7]
pCN004	pKAS32 <i>lacZ:P<sub>tac</sub>-mKate2:lacZ</i>	[8]
pCN007	pKAS32 $\Delta$ <i>rbmA</i>	[9]
pCN008	pKAS32 $\Delta$ <i>rbmC</i>	[9]
pCN009	pKAS32 $\Delta$ <i>bapI</i>	[3]
pCDN010	pKAS32 $\Delta$ <i>pomA</i>	[9]
pEXG2	Allelic exchange vector with pBR origin, gentamicin resistance, <i>sacB</i>	[10]

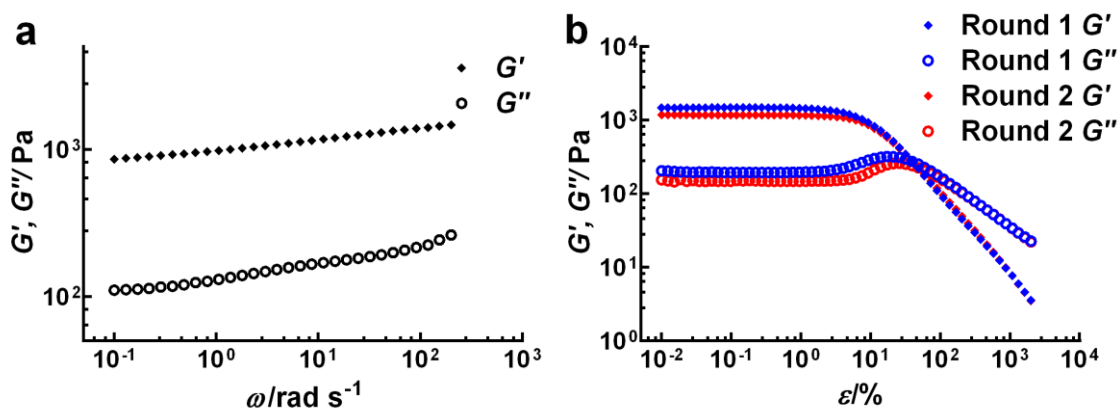


Figure S1. *V. cholerae* biofilms behave as hydrogels. a) Storage modulus  $G'$  (filled diamonds) and loss modulus  $G''$  (open circles) of WT *V. cholerae* biofilms grown for two days on plates with 0.6% agar, as a function of frequency  $\omega$ , measured in a parallel-plate geometry. b) Storage modulus  $G'$  and loss modulus  $G''$  of the same *V. cholerae* biofilm samples as a function of the amplitude of oscillatory shear strain  $\epsilon$ . The red curves were measured immediately after the blue curves. Irreversible structural changes during yielding cause a modest decrease in both  $G'$  and  $G''$  in the second round of measurements.

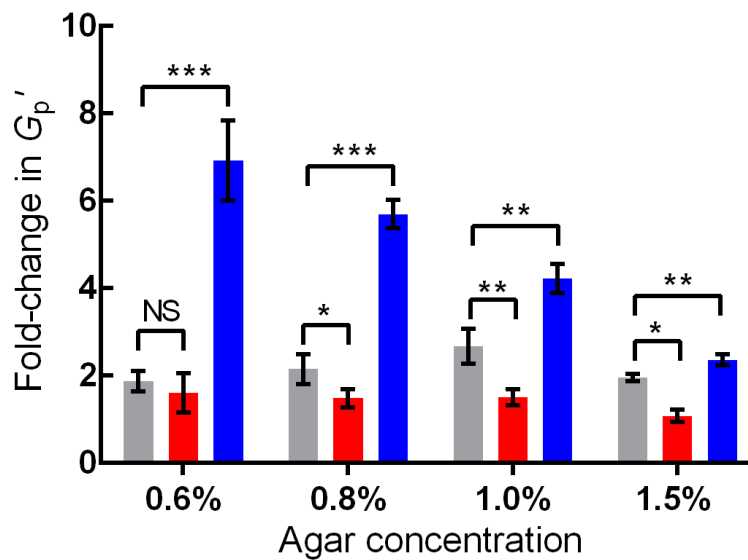


Figure S2. RbmA-mediated cell-cell connections strengthen biofilms in a VPS and RbmC/Bap1-dependent manner. Plotted are fold-changes in  $G'_p$  in biofilms made of cells possessing *rbmA* compared to those lacking *rbmA* that are otherwise WT (gray),  $\Delta vpsL$  (red), and  $\Delta bap1\Delta rbmC$  (blue). The bacterial strains were grown on plates with the designated agar concentrations. NS stands for not significant; \* denotes  $P < 0.05$ , \*\* denotes  $P < 0.01$ , \*\*\* denotes  $P < 0.001$ . Error bars correspond to standard deviations with  $n = 3$ . In the absence of VPS, RbmA cannot mediate cell-cell connections to increase  $G'_p$  (i.e. red bars are not significantly different from a value = 1). This result is consistent with previous microscopy results showing that the retention of RbmA in a *V. cholerae* biofilm requires VPS.<sup>[11]</sup> On the other hand, in the absence of RbmC/Bap1, the strengthening effect of RbmA-mediated cell-cell connections is amplified compared to its strengthening effect in the WT (compare blue to gray bars).

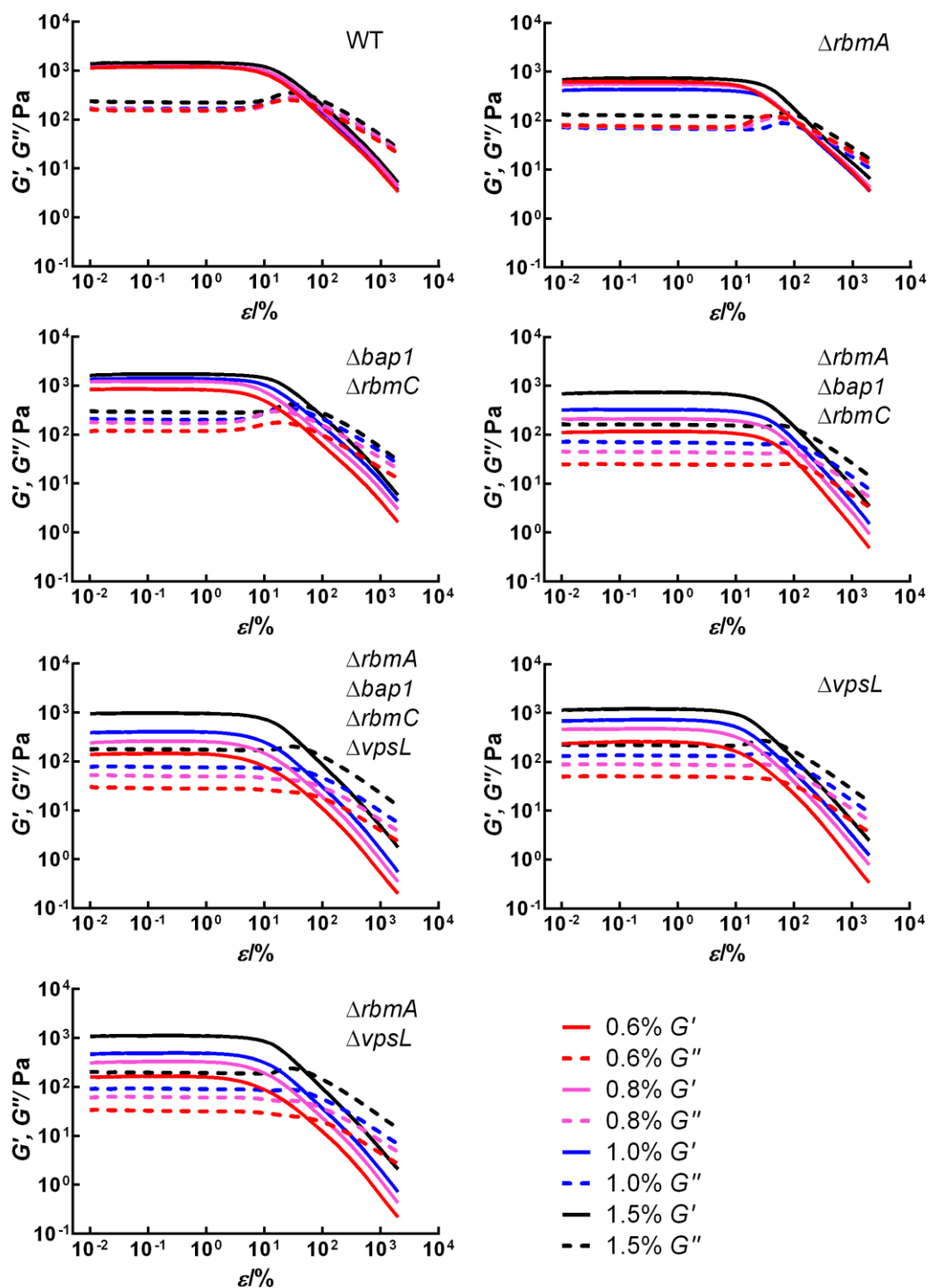


Figure S3. Complete rheological data for main Figures 1-2, Figure S2, and Table S1. Shown are the storage modulus  $G'$  (solid curves) and loss modulus  $G''$  (dashed curves) as a function of the amplitude of oscillatory strain  $\epsilon$  for the *V. cholerae* strains indicated on the plots.

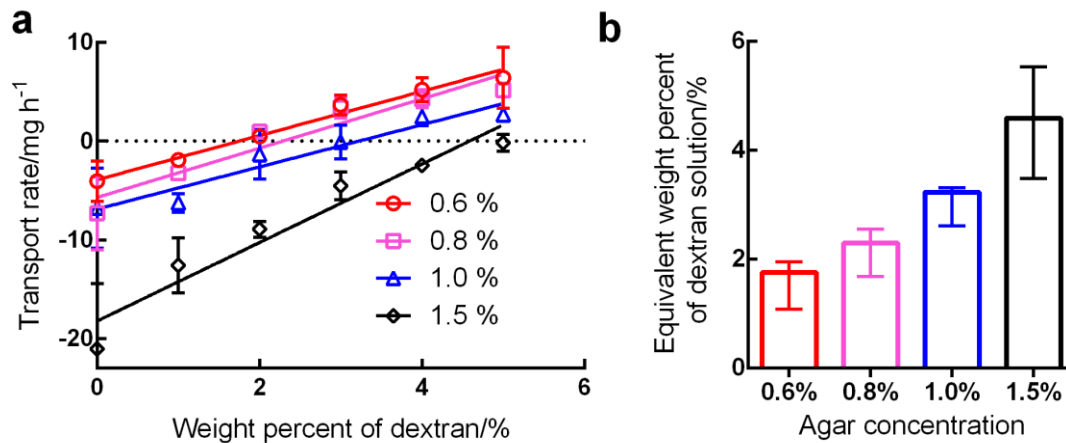


Figure S4. Measurement of osmotic pressures of agar substrates. a) A droplet of LB medium containing dextran was placed on a semi-permeable membrane on top of different concentration agar substrates (0.6-1.5%). Depending on the dextran concentration in the droplet and the agar concentration in the substrate, an osmotic contrast is established across the semi-permeable membrane. Thus, the liquid droplet either takes up water from the agar or loses water to the agar. Using linear interpolation, we identified the concentration of dextran at which there is zero net flow across the membrane. We used these values as proxies for the osmotic pressures of the agar at each concentration, shown in (b). Importantly, we find that the osmotic pressure of agar plates is equivalent to polymer concentrations between 1-5%, which is on the order of the matrix polysaccharide concentration in the biofilm.<sup>[3]</sup> Specifically, in our earlier contribution, we found that the volume fraction of the vibrio polysaccharide matrix is  $\sim$  1-4% of the extracellular biofilm space.<sup>[3]</sup> Therefore, depending on the agar concentration, the biofilm matrix will either take up or lose water,<sup>[3, 12]</sup> similar to the dextran droplet in the above experiments. Error bars correspond to standard deviations in (a) and 95% confidence intervals in (b).

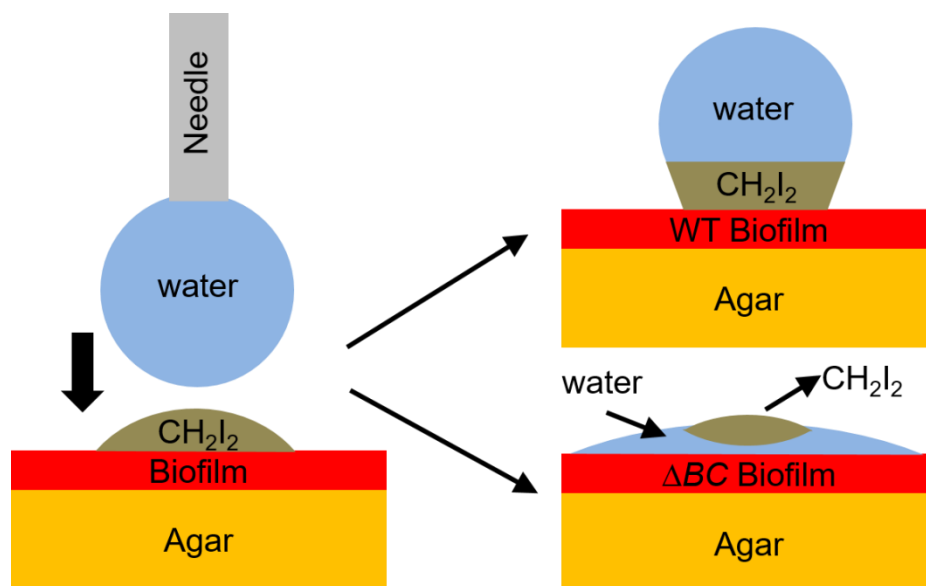


Figure S5. Schematic representation of the experiment in main Figure 3c. Not drawn to scale. Depending on the polarity of the biofilm, either water or CH<sub>2</sub>I<sub>2</sub> is in preferential contact with the biofilm.



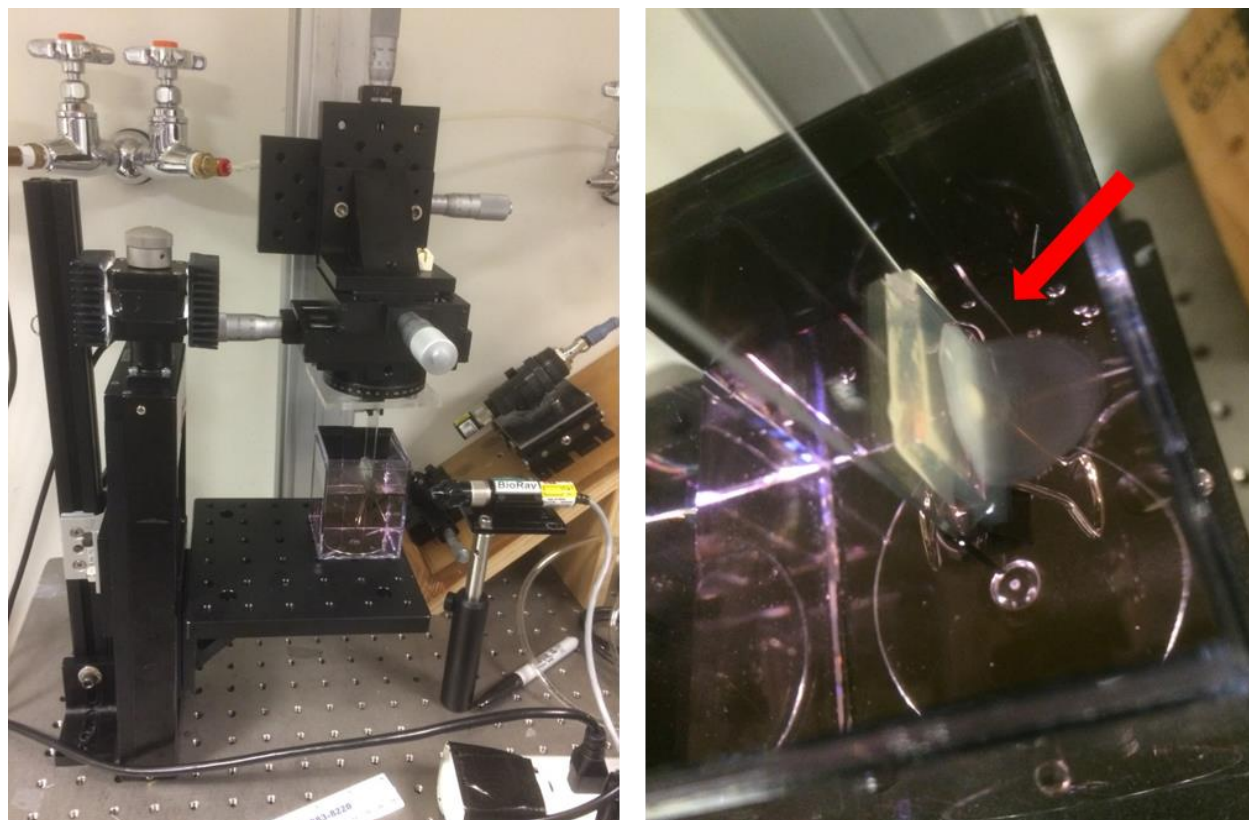


Figure S6. *Left*: Image of the experimental setup for capillary peeling with controlled peeling velocity. *Right*: Close-up view of the biofilm. The red arrow indicates the position of the *V. cholerae* biofilm. Half of the biofilm has been peeled off and floats on the water while the other half remains adhered to the agar substrate.

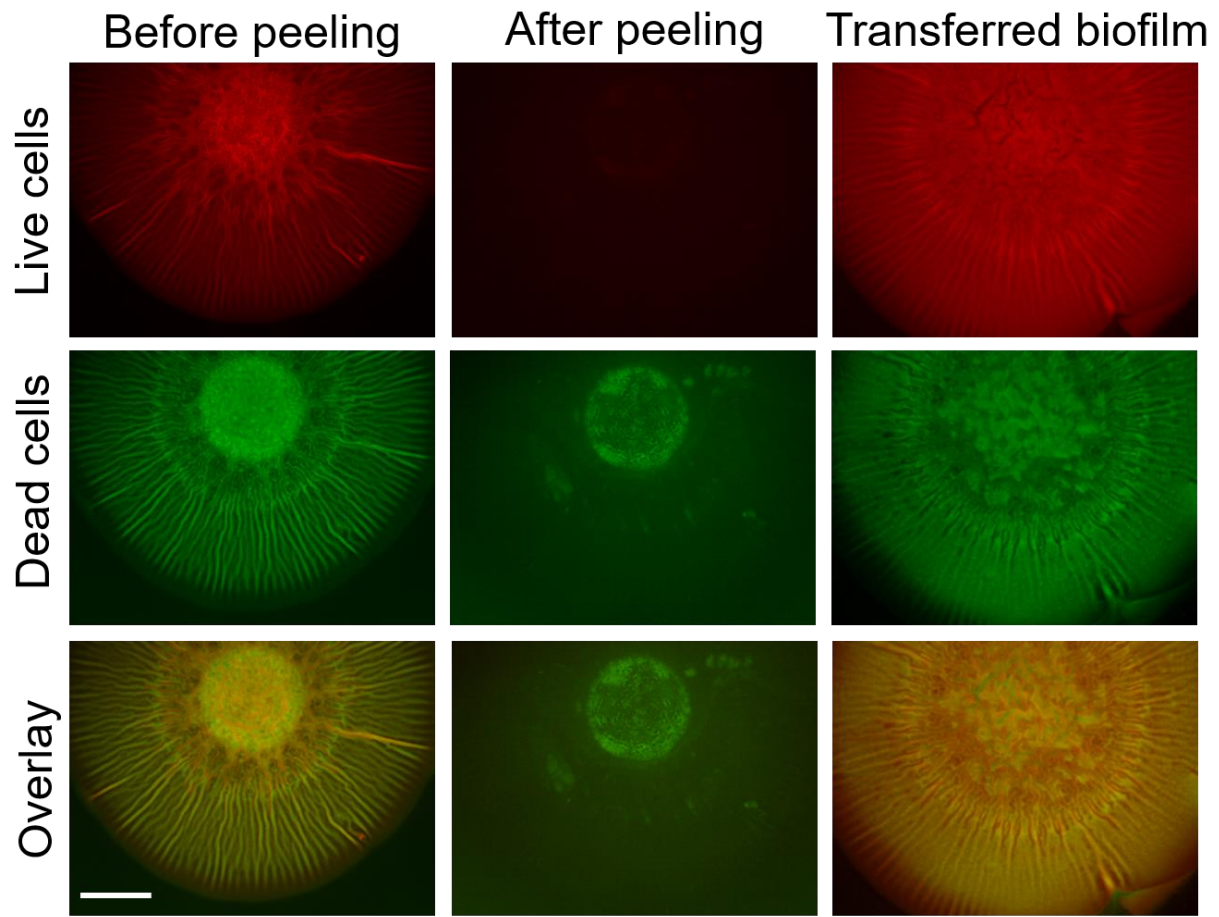


Figure S7. Capillary peeling as a biofilm removal and transfer technique. Shown are fluorescence images of the agar substrate (0.6%) before (*left*) and after (*middle*) capillary removal of a WT *V. cholerae* biofilm, as well as the images of the transferred biofilm (*right*). Red (*top*) is fluorescence from mKate2 in live cells. Green (*middle*) corresponds to SytoX DNA staining of dead cells. *Bottom* row shows images by overlaying the red and green channels. Scale bar: 3 mm.

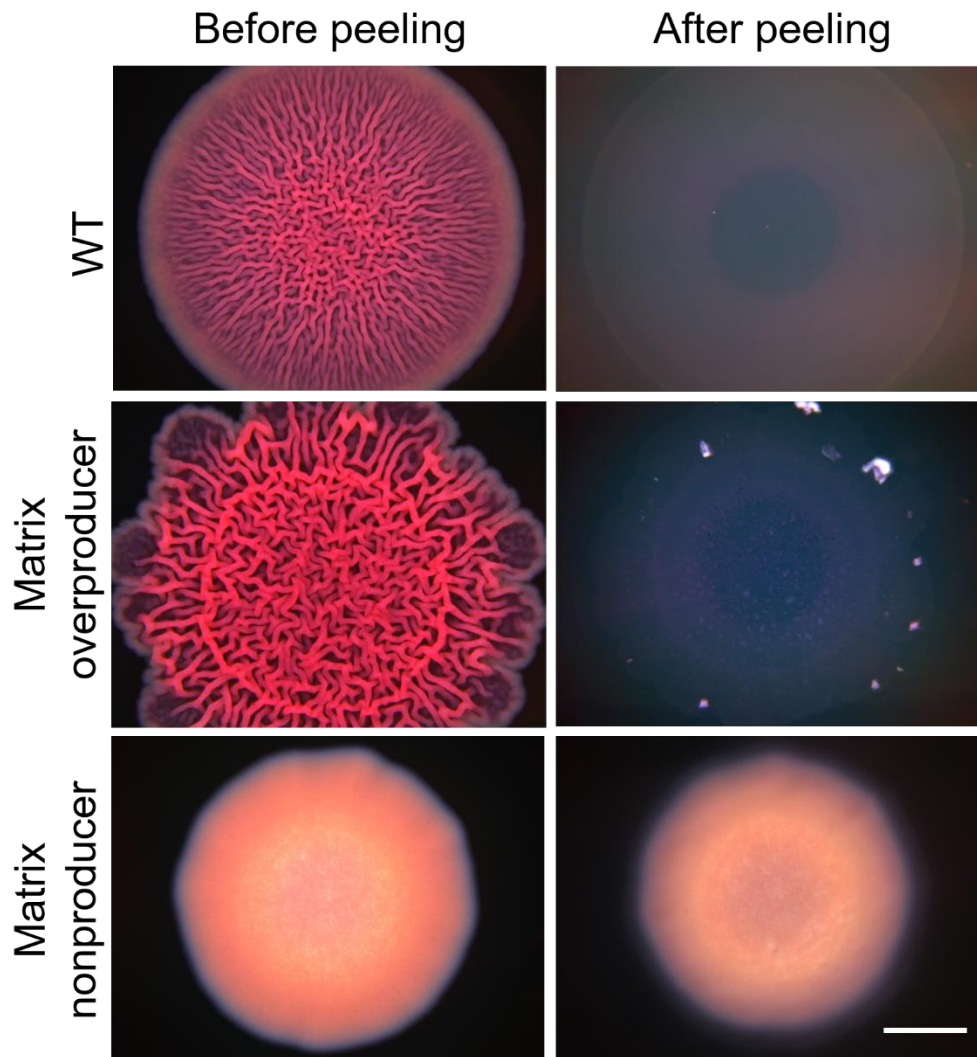


Figure S8. Capillary peeling of *Pseudomonas aeruginosa* biofilms grown on 1.0% agar substrates containing congo red dye. Images of the biofilms taken before peeling are shown on the *left* and images of the agar substrates after peeling are shown on the *right*. From *top* to *bottom* are biofilms of WT *P. aeruginosa* PA14, a *P. aeruginosa* PA14 strain that overproduces the Pel matrix polysaccharide, and a *P. aeruginosa* PA14 strain that lacks Pel (See Table S3 for details). *P. aeruginosa* biofilms can only be peeled off an agar substrate if the strain produces the matrix polysaccharide. Scale bar: 3 mm.

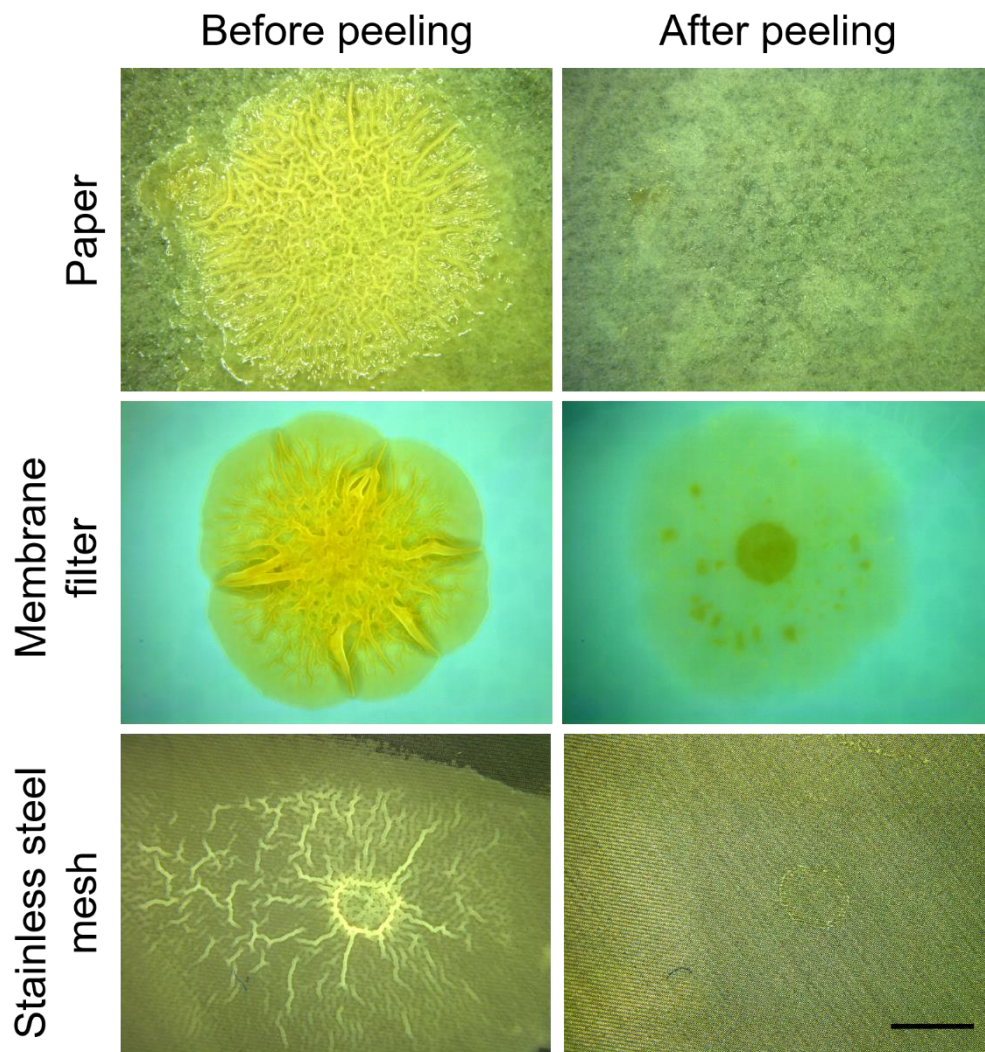


Figure S9. Application of the capillary peeling method to *V. cholerae* biofilms grown on different substrates (See Methods for growth conditions). Biofilm images before peeling are shown on the *left* and surface images after peeling are shown on the *right*. Scale bar: 3 mm.

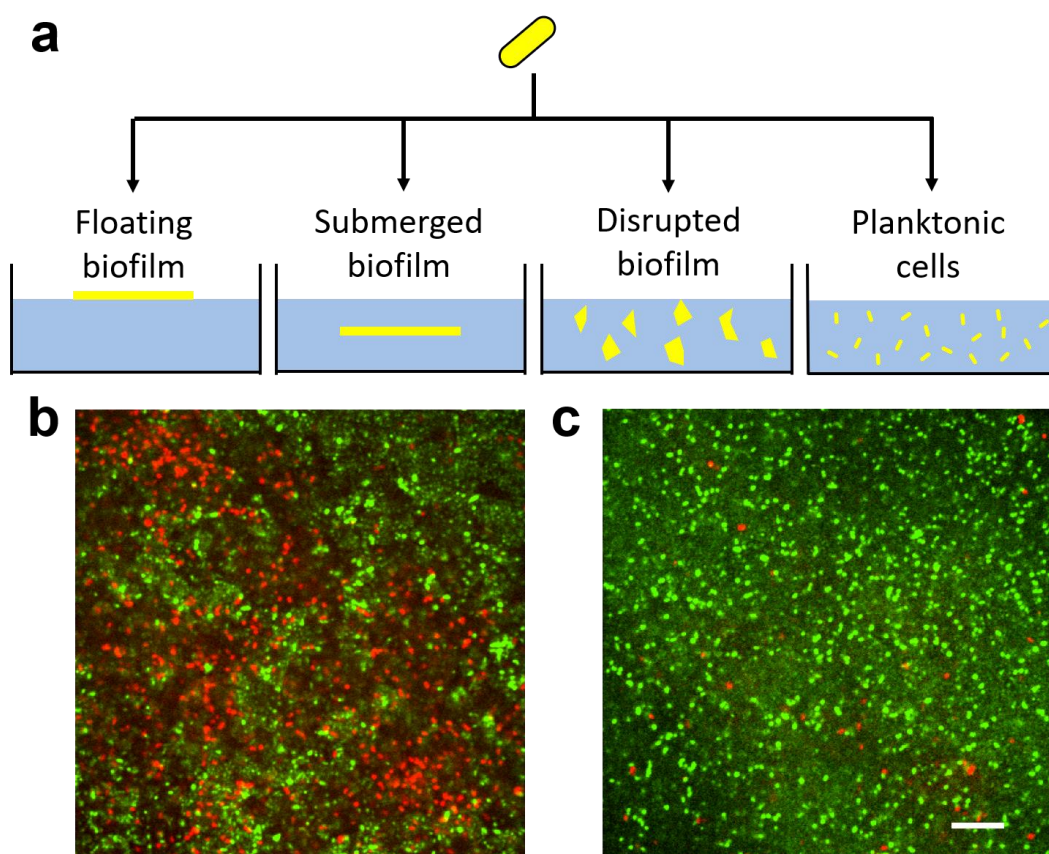


Figure S10. Application of the biofilm transfer technique. a) Schematic representation of the experiment in main Figure 5c. Yellow denotes *V. cholerae* cells. Blue denotes the liquid LB medium containing the antibiotic (tetracycline at  $50 \mu\text{g mL}^{-1}$ ). Not drawn to scale. b,c) Confocal microscopy images of live-dead staining of biofilm-dwelling cells. Green and red signals correspond to live cells and dead cells, respectively. For panels b and c, a WT *V. cholerae* biofilm was grown for two days on a plate containing 0.6% agar. Subsequently, the biofilm was peeled off the agar substrate via the capillary peeling method (left-most schematic in panel a), and floated on LB medium containing tetracycline. After 1 h of antibiotic treatment, the floating biofilm was transferred to a #1.5 glass coverslip with the original base of the biofilm attached to the coverslip (via the *right* configuration in main text Figure 5a). The biofilm was imaged from the bottom through the coverslip. Panel b shows the base of the biofilm and panel c shows an image taken  $10 \mu\text{m}$  above the biofilm base. Scale bar:  $10 \mu\text{m}$ .

**Supplementary Methods: Principles of surface energy measurements**

The calculation of surface energy follows the original manuscript by Owens and Wendt,<sup>[13]</sup> which is briefly summarized here. The surface energy of a biofilm  $\gamma_f$  can be decomposed into the nonpolar, dispersion force component  $\gamma_f^d$  and the polar component due to hydrogen bonding and/or dipole-dipole forces  $\gamma_f^p$ ,

$$\gamma_f = \gamma_f^d + \gamma_f^p \quad (1)$$

The interfacial energy  $\gamma_{fl}$  between a biofilm and a liquid (l) located on top of the biofilm follows:

$$\gamma_{fl} = (\sqrt{\gamma_f^d} - \sqrt{\gamma_l^d})^2 + (\sqrt{\gamma_f^p} - \sqrt{\gamma_l^p})^2 \quad (2)$$

in which  $\gamma_l^d$  and  $\gamma_l^p$  are the dispersion and polar components of the surface energy of the liquid, respectively. Neglecting the vapor pressure effect, the Young equation for a liquid droplet located on top of a biofilm is:

$$\gamma_l \cos \theta = \gamma_f - \gamma_{fl} \quad (3)$$

where  $\theta$  is the contact angle. Combining equations (2) and (3), one arrives at the expression:

$$1 + \cos \theta = 2\sqrt{\gamma_f^d} \left( \frac{\sqrt{\gamma_f^d}}{\gamma_l} \right) + 2\sqrt{\gamma_f^p} \left( \frac{\sqrt{\gamma_f^p}}{\gamma_l} \right) \quad (4)$$

Therefore, by measuring the contact angle  $\theta$  of two liquids with known  $\gamma_l^d$ ,  $\gamma_l^p$ , and  $\gamma_l$ , against a biofilm, simultaneous equations are obtained which can be used to solve for  $\gamma_f^d$  and  $\gamma_f^p$ . We chose water and CH<sub>2</sub>I<sub>2</sub> as the test liquids and used the surface energy values reported in the original manuscript by Owens and Wendt.<sup>[13]</sup>

**SI Movie Caption**

Video S1: Capillary peeling of a WT *V. cholerae* biofilm grown on a 0.6% agar substrate for two days and subsequent pick-up with a glass substrate. The movie is played in real time.

**Supplementary Reference**

- [1] V. De Lorenzo, K. N. Timmis, *Methods Enzymol.* **1993**, 235, 386.
- [2] K. H. Thelin, R. K. Taylor, *Infect. Immun.* **1996**, 64, 2853.
- [3] J. Yan, C. D. Nadell, H. A. Stone, N. S. Wingreen, B. L. Bassler, *Nat. Commun.* **2017**, 8, 327.
- [4] S. Mukherjee, D. Moustafa, C. D. Smith, J. B. Goldberg, B. L. Bassler, *PLOS Pathog.* **2017**, 13, e1006504.
- [5] K. Skorupski, R. K. Taylor, *Gene* **1996**, 169, 47.
- [6] K. Drescher, C. D. Nadell, H. A. Stone, N. S. Wingreen, B. L. Bassler, *Curr. Biol.* **2014**, 24, 50.
- [7] B. K. Hammer, B. L. Bassler, *Mol. Microbiol.* **2003**, 50, 101.
- [8] C. D. Nadell, B. L. Bassler, *Proc. Natl. Acad. Sci. USA* **2011**, 108, 14181.
- [9] C. D. Nadell, K. Drescher, N. S. Wingreen, B. L. Bassler, *ISME J.* **2015**, 9, 1700.
- [10] L. R. Hmelo, B. R. Borlee, H. Almblad, M. E. Love, T. E. Randall, B. S. Tseng, C. Lin, Y. Irie, K. M. Storek, J. J. Yang, R. J. Siehnel, P. L. Howell, P. K. Singh, T. Tolker-Nielsen, M. R. Parsek, H. P. Schweizer, J. J. Harrison, *Nat. Protoc.* **2015**, 10, 1820.
- [11] a) V. Berk, J. C. N. Fong, G. T. Dempsey, O. N. Develioglu, X. W. Zhuang, J. Liphardt, F. H. Yildiz, S. Chu, *Science* **2012**, 337, 236; b) J. Yan, A. G. Sharo, H. A. Stone, N. S. Wingreen, B. L. Bassler, *Proc. Natl. Acad. Sci. USA* **2016**, 113, E5337.
- [12] A. Seminara, T. E. Angelini, J. N. Wilking, H. Vlamakis, S. Ebrahim, R. Kolter, D. A. Weitz, M. P. Brenner, *Proc. Natl. Acad. Sci. USA* **2012**, 109, 1116.
- [13] D. K. Owens, R. C. Wendt, *J. Appl. Polym. Sci.* **1969**, 13, 1741.